

The contact dynamics method for granular media

Tamás Unger* and János Kertész*

**Department of Theoretical Physics, Budapest University of Technology and Economics, H-1111
Budapest, Hungary*

Abstract. In this paper we review the simulation method of the *non-smooth contact dynamics*. This technique was designed to solve the unilateral and frictional contact problem for a large number of rigid bodies and has proved to be especially valuable in research of dense granular materials during the last decade. We present here the basic principles compared to other methods and the detailed description of a 3D algorithm. We point out an artifact manifesting itself in spurious sound waves and discuss the applicability of the method.

INTRODUCTION

Granular materials, due to their rich phenomenology and wide variety of applications in technological processes, have captured much recent interest and are subject of active research. Their study is often based on computer simulations, where, with growing importance, *discrete element methods* play a fundamental role. Such numerical techniques, e.g. the well known soft particle *molecular dynamics* [1, 2], the *event driven method* [3, 2] or the here presented *non-smooth contact dynamics* [4, 5, 2, 6], have the common property that the trajectory of each single particle is calculated by virtue of interaction with other particles and with the environment. The characteristics of these algorithms originate mainly from different treatments of interparticle interactions, which leads to somewhat different applicabilities. E.g. the event driven method operates with instant binary collisions and works very well in gas-like situations, however, if a dense state is approached, where clusters of contacting grains would appear, then the simulation gets critically slow, a phenomenon known as *inelastic collapse*[3].

The simulation of dense granular systems is always a computational challenge, in a typical situation dry friction and many long lasting contacts between hard particles have to be taken into account. Using *molecular dynamics* (MD) the velocities are modeled as smooth functions of time (even for collisions), therefore the treatment of hard bodies becomes problematic: here small time steps of the integration must be used resulting in slow simulation. As we will see later, this problem of numerous hard particles is difficult to solve even with other conceptions. In MD further difficulties are encountered by dry friction, where it is not obvious how to distinguish between sliding and nonsliding contacts.

The *contact dynamics* method (CD), developed by M. Jean and J. J. Moreau [4, 5, 6], has a clear conception to overcome the above mentioned difficulties. The way is to consider the particles as perfectly rigid and to handle the interaction by means of

the perfect volume exclusion, i.e. the contacting bodies may not deform each other. For that an implicit algorithm is used, which has the significant advantage that the implementation of dry friction is rather simple; the infinitely steep graph of Coulomb friction can be adopted, thus no regularization is needed. The resulting method provides realistic dynamics for various granular systems and is especially efficient for simulating frictional multi-contact situations of hard bodies (for comparison with experiments and with other methods see [7, 8, 9]).

Although in recent years CD has been the simulation tool of many studies [10, 11, 12, 13] that provided understanding for several questions of granular media, it is rather difficult to implement this algorithm relying merely on the literature. The reason, it seems to us, is the lack of a practical description with hints how to adopt CD. One of the goals of this paper is to help solving this problem: in the following section the basic ideas and the structure of our 3D CD algorithm is presented. The description here is confined mostly to cohesionless, rigid and spherical particles with perfectly inelastic collisions (i.e. with zero Newton restitution), but it has to be emphasized that CD contains no restriction on shape or on other of these conditions. We refer to simulations, where cohesive disks and polygons were implemented [13, 14], or particles with finite Newton restitution [8], even deformable bodies can be adopted in CD with a minor change of variable [6].

Finally we will discuss some consequences of the *iterative solver* used for the calculation of the interparticle forces (see later) with respect to the computational time and we will review a potential elastic behavior that may arise from inaccurate force-determination.

THE CD METHOD

The basic principles

As a *discrete element method* CD provides the dynamics by integrating the equations of motion for each particle, where besides external fields (e.g. gravity) the interaction between the particles are also taken into account. The particles are considered as perfectly rigid and interact with each other via point-contacts. The question is, how the force at such a contact is calculated with CD. Because of the rigidity it cannot be given as a function of the extent or rate of the contact-deformation, like in the case of the soft particle MD. In fact, the principles of the two methods are basically different. In CD the contact forces are calculated by virtue of their effect, namely the generated motion has to fulfill certain constraints. Typically such a constraint is the volume exclusion of the particles, or the absence of sliding due to static friction.

Using constraint forces for the interaction has a serious consequence: a contact force depends also on other forces that press the two contacting bodies together, e.g. on adjacent contact forces. Thus for a compressed cluster of rigid particles the problem cannot be solved locally for each contact. In the algorithm, in order to calculate a global consistent system of constraint forces at every time step, an iterative scheme is needed (called the *iterative solver*).

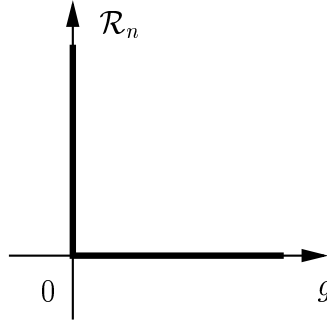


FIGURE 1. The Signorini graph

This iteration process of course demands computational effort, but in exchange it makes possible to apply an implicit stepping algorithm with large time steps. The resulting dynamics is non-smooth and includes velocity jumps due to shocks when collisions occur. In contrast, the MD method considers the motion smooth even for collision, therefore the harder the particles are, the finer resolution in time is needed, consequently small time steps are used.

The constraint conditions

The main feature of unilateral contacts we want to attain is impenetrability, furthermore only repulsive forces are allowed corresponding to dry granular materials. This is expressed by the Signorini graph (Fig. 1), which relates the gap g between two particles and the normal force \mathcal{R}_n between them. \mathcal{R}_n can be non-negative and arbitrarily large if $g = 0$, but becomes zero if the two particles are not in contact ($g > 0$). In the algorithm the normal force is determined according to this multi-mapping graph and to the additional principle, that the smallest value of \mathcal{R}_n is applied at a contact, which is just needed to avoid interpenetration.

Regarding the tangential force \mathcal{R}_t it is due to the Coulomb friction (Fig. 2), which captures the characteristics of dry frictional contacts that sliding cannot be induced below a certain threshold. This threshold is proportional to the normal force with the factor μ , the friction coefficient. (Here we neglect the difference between static and sliding friction coefficients for simplicity, but this distinction can be made in CD without difficulty.)

In a non-sliding situation the value of \mathcal{R}_t is not determined by the graph, the static friction force can be arbitrary below the threshold. Here a similar constraint principle is applied as for \mathcal{R}_n , namely that the proper friction force is chosen, which is needed to keep the contact from sliding. If this condition cannot be satisfied below the threshold, then the contact will slide with a friction force $\mu\mathcal{R}_n$ against the motion, i.e. pointing opposite to the relative tangential velocity.

The graph shown in Figure 2 concerns rather a two-dimensional case. In three-dimension one can speak about the Coulomb cone: for a given \mathcal{R}_n the friction force

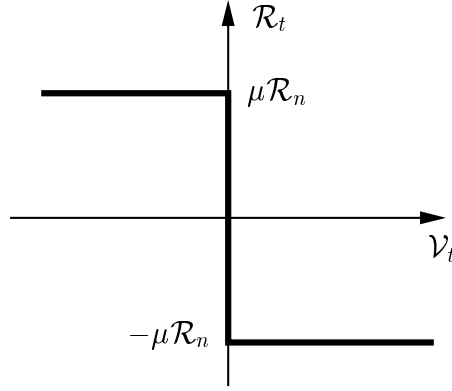


FIGURE 2. The Coulomb graph

must lie in a two-dimensional plane within a circle, the radius of which is defined by the threshold above, thus the radius depends linearly on the normal force.

We would like to emphasize that both graphs presented here are infinitely steep and can be implemented in the CD method without any change.

The discrete dynamical equations

According to the Signorini condition, collisions of particles give rise to shocks, therefore discontinuous velocities are expected during the time-evolution. In such a case of non-smooth mechanics [15] the use of second or higher order schemes for the integration of motion is not beneficial and could even be problematic. Therefore first order schemes are applied, e.g. an implicit Euler integration in our CD code:

$$\vec{r}_i(t + \Delta t) = \vec{r}_i(t) + \vec{v}_i(t + \Delta t) \Delta t \quad (1)$$

$$\vec{v}_i(t + \Delta t) = \vec{v}_i(t) + \frac{1}{m_i} \vec{F}_i(t + \Delta t) \Delta t. \quad (2)$$

The two equations describe the change in velocity and position of the center of mass during one time step for the i th particle. The vector \vec{F}_i denotes the sum of the forces acting on this particle and is calculated to be consistent with the new velocities and positions.

The time-stepping is also similar for the rotation around the center of mass: the orientation of a particle is updated with the new angular velocity $\vec{\omega}_i(t + \Delta t)$, while for the update of $\vec{\omega}_i$ we use the torque $\vec{T}_i(t + \Delta t)$ resulting from the new contact forces.

One contact

Let us first consider the simple case of only one candidate for contact, i.e. two convex particles already in contact or with a small gap between them. They are numbered 0

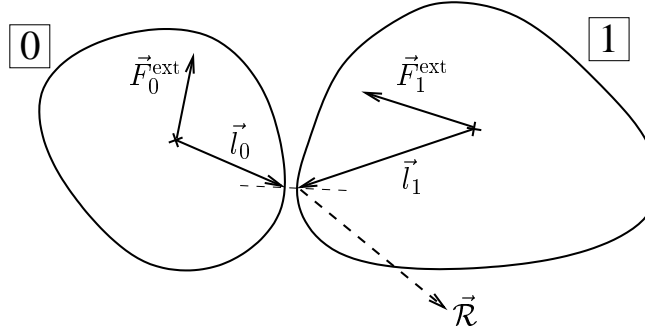


FIGURE 3. Two rigid particles before a possible contact state.

and 1 and may be subjected to constant external forces $\vec{F}_0^{\text{ext}}, \vec{F}_1^{\text{ext}}$ acting on the centers of mass (Fig. 3). The volume exclusion and the Coulomb friction law may require a constraint force $\vec{\mathcal{R}}$ at this contact-candidate (contact force for short), where we use the convention that $\vec{\mathcal{R}}$ acts on particle 1, while its reaction force $-\vec{\mathcal{R}}$ acts on the other one. In this section we will show how $\vec{\mathcal{R}}$ is calculated with *contact dynamics*.

An important quantity of a contact-candidate is its relative velocity:

$$\vec{\mathcal{V}} = \vec{v}_1 + \vec{\omega}_1 \times \vec{l}_1 - (\vec{v}_0 + \vec{\omega}_0 \times \vec{l}_0), \quad (3)$$

where the vectors \vec{l}_0 and \vec{l}_1 point from the centers of mass to possible contact points.

It is useful to introduce a generalized velocity vector:

$$\mathbf{V} = \begin{bmatrix} \vec{v}_0 \\ \vec{\omega}_0 \\ \vec{v}_1 \\ \vec{\omega}_1 \end{bmatrix}. \quad (4)$$

With the bold notation we indicate that \mathbf{V} is not a three-dimensional vector but actually has 12 real components. The form (3) shows a linear dependence of the contact velocity $\vec{\mathcal{V}}$ on \mathbf{V} .

In a similar way generalized forces can be defined:

$$\mathbf{R} = \begin{bmatrix} \vec{R}_0 \\ \vec{T}_0 \\ \vec{R}_1 \\ \vec{T}_1 \end{bmatrix} \quad \mathbf{F}^{\text{ext}} = \begin{bmatrix} \vec{F}_0^{\text{ext}} \\ \vec{0} \\ \vec{F}_1^{\text{ext}} \\ \vec{0} \end{bmatrix}, \quad (5)$$

where \mathbf{R} contains torques and central forces equivalent to the effect of $\vec{\mathcal{R}}$:

$$\vec{R}_0 = -\vec{\mathcal{R}}, \quad \vec{R}_1 = \vec{\mathcal{R}}, \quad \vec{T}_0 = -\vec{l}_0 \times \vec{\mathcal{R}}, \quad \vec{T}_1 = \vec{l}_1 \times \vec{\mathcal{R}}, \quad (6)$$

while \mathbf{F}^{ext} collects the external forces (the external torques are zero).

Now the relation between the corresponding contact and central quantities can be expressed with the following linear forms:

$$\mathbf{R} = \mathbf{H}\vec{\mathcal{R}} \quad (7)$$

$$\vec{\gamma} = \mathbf{H}^T \mathbf{V}, \quad (8)$$

where \mathbf{H}^T is the transpose of the matrix \mathbf{H} . These two matrices depend only on the geometry, their structures follow from Eq. (3) and Eq. (6):

$$\mathbf{H} = \begin{bmatrix} -\mathbf{1} \\ -(\vec{l}_0 \times) \\ \mathbf{1} \\ (\vec{l}_1 \times) \end{bmatrix}, \quad (9)$$

$$\mathbf{H}^T = \begin{bmatrix} -\mathbf{1} & (\vec{l}_0 \times) & \mathbf{1} & -(\vec{l}_1 \times) \end{bmatrix}. \quad (10)$$

The elements here are 3×3 matrices: $\mathbf{1}$ is the unit matrix and $(\vec{l}_i \times)$ gives simply the crossproduct of \vec{l}_i and the vector it is acting on. The matrix \mathbf{H} allows us to transform contact quantities into particle quantities and vice versa.

For the particles Newton's equation of motion reads:

$$\frac{d\mathbf{V}}{dt} = \mathbf{M}^{-1} \mathbf{R} + \mathbf{M}^{-1} \mathbf{F}^{\text{ext}}, \quad (11)$$

where \mathbf{M}^{-1} is the inverse of the generalized mass matrix, which is built up from the masses and moments of inertia matrices of the particles:

$$\mathbf{M} = \begin{bmatrix} m_0 \mathbf{1} & 0 & 0 & 0 \\ 0 & \mathbf{I}_0 & 0 & 0 \\ 0 & 0 & m_1 \mathbf{1} & 0 \\ 0 & 0 & 0 & \mathbf{I}_1 \end{bmatrix}. \quad (12)$$

If one transforms the Equation (11) multiplying it with \mathbf{H}^T from the left, the equation of motion can be obtained regarding this candidate for contact (note that the term $d\mathbf{H}^T/dt \mathbf{V}$ describing the geometrical change is neglected here, which is typically a good approximation) :

$$\frac{d\vec{\gamma}}{dt} = \mathcal{M}^{-1} \vec{\mathcal{R}} + \frac{d\vec{\gamma}^{\text{free}}}{dt}, \quad (13)$$

where \mathcal{M} is the effective mass matrix of the contact and it describes the contact-acceleration due to the contact force. This is an important relation because, as we will see, it gives the possibility to utilize our constraint conditions and therefore to calculate the interparticle force $\vec{\mathcal{R}}$.

The second term of the right hand side in Eq. (13) has the meaning of the acceleration without any interaction between the particles, i.e. only due to the external forces:

$$\frac{d\vec{\mathcal{V}}^{\text{free}}}{dt} = \mathbf{H}^T \mathbf{M}^{-1} \mathbf{F}^{\text{ext}} \quad (14)$$

The properties of the effective mass matrix \mathcal{M}

The value of \mathcal{M}^{-1} easily follows from the transformations (7) and (8):

$$\mathcal{M}^{-1} = \mathbf{H}^T \mathbf{M}^{-1} \mathbf{H} . \quad (15)$$

It can be shown that \mathcal{M}^{-1} gets a really simple form for contacting spheres, because on one hand the spherical moments of inertia simplify \mathcal{M}^{-1} (i.e. I_0 and I_1 are numbers):

$$\mathcal{M}^{-1} = \left(\frac{1}{m_0} + \frac{1}{m_1} + \frac{\vec{l}_0^2}{I_0} + \frac{\vec{l}_1^2}{I_1} \right) \mathbf{1} - \frac{1}{I_0} (\vec{l}_0 \circ \vec{l}_0) - \frac{1}{I_1} (\vec{l}_1 \circ \vec{l}_1) \quad (16)$$

(where \circ is the dyadic product), on the other hand one can take into account the fact that \vec{l}_0 and \vec{l}_1 are on the same line, which is perpendicular to the contact surface. The result is that \mathcal{M}^{-1} can be characterized by two parameters m_n and m_t :

$$m_n = \left(\frac{1}{m_0} + \frac{1}{m_1} \right)^{-1} \quad (17)$$

$$m_t = \left(\frac{1}{m_n} + \frac{\vec{l}_0^2}{I_0} + \frac{\vec{l}_1^2}{I_1} \right)^{-1} , \quad (18)$$

which could be called normal and tangential mass respectively, as they are the inertia of this candidate in normal and tangential direction. More clearly if $\vec{\mathcal{R}}$ is given by the sum of the normal and tangential component: $\mathcal{R}_n \vec{n} + \vec{\mathcal{R}}_t$ (\vec{n} is a normal unit vector, while the tangential component is a vector in the two-dimensional tangent plane), then \mathcal{M}^{-1} acts in the following way:

$$\mathcal{M}^{-1} \vec{\mathcal{R}} = \frac{1}{m_n} \mathcal{R}_n \vec{n} + \frac{1}{m_t} \vec{\mathcal{R}}_t . \quad (19)$$

Thus the normal and tangential components are not coupled for spheres, which is not true in general.

The time stepping

Turning back to the dynamics, our aim is to find a proper interaction force in accordance with the discrete equations. Based on the implicit Euler scheme, the following

discrete form of the dynamical equations is obtained for the two-particle system:

$$\mathbf{V}^{\text{new}} - \mathbf{V} = (\mathbf{M}^{-1} \mathbf{R}^{\text{new}} + \mathbf{M}^{-1} \mathbf{F}^{\text{ext}}) \Delta t . \quad (20)$$

The superscript “new” indicates the yet unknown values of parameters, i.e. the values after the time step Δt . Because the external forces are kept constant here, their change is not involved in the equation. This implies the following approximate change in contact velocity during one time step:

$$\vec{\mathcal{V}}^{\text{new}} - \vec{\mathcal{V}} = \left(\mathcal{M}^{-1} \vec{\mathcal{R}}^{\text{new}} + \mathbf{H}^T \mathbf{M}^{-1} \mathbf{F}^{\text{ext}} \right) \Delta t , \quad (21)$$

where the unknown values are $\vec{\mathcal{V}}^{\text{new}}$ and $\vec{\mathcal{R}}^{\text{new}}$. The part of this velocity change due to the external forces is known and can be subtracted from Eq. (21):

$$\vec{\mathcal{V}}^{\text{new}} - \vec{\mathcal{U}} = \mathcal{M}^{-1} \vec{\mathcal{R}}^{\text{new}} \Delta t , \quad (22)$$

where

$$\vec{\mathcal{U}} = \mathbf{H}^T \mathbf{M}^{-1} \mathbf{F}^{\text{ext}} \Delta t + \vec{\mathcal{V}} \quad (23)$$

would be the new velocity without interaction.

Similarly, positions are updated by means of new velocities (Eq. 1), which implies the following predictive formula for the gap g (the distance between the two particles):

$$g^{\text{new}} - g = \mathcal{V}_n^{\text{new}} \Delta t , \quad (24)$$

where $\mathcal{V}_n^{\text{new}} = \vec{n} \vec{\mathcal{V}}^{\text{new}}$ is the normal component of the contact velocity. The normal vector \vec{n} points from particle 0 towards particle 1, thus for approaching particles the normal velocity is negative. Note, that negative g has the meaning of an overlap.

Considering the Equations (22) and (24) the constraint conditions can be easily imposed on the “new” situation, which is done in three steps in the algorithm:

1. First we check what happens to the gap without interaction after Δt and if it remains positive:

$$g + \mathcal{U}_n \Delta t > 0 , \quad (25)$$

then $\vec{\mathcal{R}}^{\text{new}}$ is set to zero. This means if the contact state is not reached no contact force is needed. If the left hand side of the inequality (25) is zero or negative, the algorithm jumps to the second point.

2. As the two objects are considered perfectly rigid, a contact force is needed to hinder the interpenetration. This step is an attempt to have a sticking contact, i.e. we require on one hand that the gap closes:

$$g^{\text{new}} = 0 , \quad (26)$$

on the other hand no slip occurs:

$$\mathcal{V}_t^{\text{new}} = 0 , \quad (27)$$

thus the unknown values can be determined. From Eq. (24) the new velocity is obtained $\vec{v}^{\text{new}} = -(g/\Delta t)\vec{n}$, then Eq. (22) reads:

$$-\frac{1}{\Delta t}\mathcal{M}\left[\left(\frac{g}{\Delta t} + \mathcal{U}_n\right)\vec{n} + \vec{\mathcal{U}}_t\right] = \vec{\mathcal{R}}^{\text{new}}, \quad (28)$$

which provides the contact force. However, this contact force can only be accepted if it satisfies the Coulomb condition:

$$\left|\vec{\mathcal{R}}_t\right| \leq \mu \mathcal{R}_n. \quad (29)$$

If this inequality does not hold, the friction is not strong enough to ensure sticking. In this case the contact will be a slipping one and a new calculation is needed for $\vec{\mathcal{R}}^{\text{new}}$, which is done in the third point.

3. For a slipping contact the condition (26) remains valid, but (27) does not. Then the following equation must be solved:

$$-\frac{1}{\Delta t}\mathcal{M}\left[\left(\frac{g}{\Delta t} + \mathcal{U}_n\right)\vec{n} + \vec{\mathcal{U}}_t - \vec{v}_t\right] = \vec{\mathcal{R}}^{\text{new}}, \quad (30)$$

together with two further conditions corresponding to the sliding friction. Firstly

$$\vec{v}_t \text{ and } \vec{\mathcal{R}}_t \text{ must be parallel and have opposite direction,} \quad (31)$$

secondly

$$\left|\vec{\mathcal{R}}_t\right| = \mu \mathcal{R}_n. \quad (32)$$

These three points form a *shock law* that in general provides the contact force at every time step. It can be applied for colliding particles, but also for an old-established contact, in that sense no distinction has to be made. If the treatment is restricted to spherical particles, the shock law can be written in a more simple form, but before the summary of this case is given, we would like to make two remarks.

Firstly, this shock law corresponds to a completely inelastic collision, i.e. to zero value of the normal restitution coefficient. To accomplish such a collision, two time steps are needed: at the first time step the relative normal velocity is only reduced but it is not set to zero, in order to let the gap close and at the following time step then the relative velocity vanishes completely for the already established contact.

Secondly, for practical applications a slight change is proposed in the shock law [6], which is the use of

$$g^{\text{pos}} = \max(g, 0) \quad (33)$$

instead of g in Equations (28) and (30). This, in principle, makes no difference because g should be non-negative. However, due to inaccurate calculations some small overlaps can be created between neighboring particles. These overlaps would be immediately eliminated by the first version of the inelastic shock law by applying larger repulsive force in order to satisfy the Equation (26). This self-correcting property, nonetheless, has the non-negligible drawback that it pumps kinetic energy into the system, while pushing

the overlapping particles apart, which mechanism can destroy stable equilibrium states. With the application of g^{pos} one gets rid of the overlap correcting impulses in such a way that the already existing overlaps are not eliminated, only the further growths are inhibited. In that sense the resulting shock law is “more inelastic” than the original one.

The inelastic shock law of the second type is given by the following very simple scheme for spherical particles, which allows different masses and sizes for the contacting spheres:

$$\begin{aligned}
& \text{if } \mathcal{U}_n \Delta t + g^{\text{pos}} > 0 \\
& \quad \text{then } \begin{cases} \mathcal{R}_n^{\text{new}} := 0 \\ \vec{\mathcal{R}}_t^{\text{new}} := 0 \end{cases} \quad (\text{no contact}) \\
& \quad \text{else } \begin{cases} \mathcal{R}_n^{\text{new}} := -\frac{1}{\Delta t} m_n \left(\frac{g^{\text{pos}}}{\Delta t} + \mathcal{U}_n \right) \\ \vec{\mathcal{R}}_t^{\text{new}} := -\frac{1}{\Delta t} m_t \vec{\mathcal{U}}_t \end{cases} \quad (\text{sticking contact}) \\
& \text{if } \left| \vec{\mathcal{R}}_t^{\text{new}} \right| > \mu \mathcal{R}_n^{\text{new}} \\
& \quad \text{then } \begin{cases} \vec{\mathcal{R}}_t^{\text{new}} := \mu \mathcal{R}_n^{\text{new}} \frac{\vec{\mathcal{R}}_t^{\text{new}}}{\left| \vec{\mathcal{R}}_t^{\text{new}} \right|} \end{cases} \quad (\text{sliding contact})
\end{aligned} \tag{34}$$

Note, that in the third sliding case the recalculation of \mathcal{R}_n is not necessary, because the mass matrix \mathcal{M} is diagonal, even the direction of the non-sliding friction force obtained before can be accepted for the sliding contact, relying on the the Eq. (22).

When situations in real experiments are numerically studied, it is a natural requirement that certain confining objects are involved in the simulation (e.g. container, fixed wall, moving piston, rotating drum). Therefore the algorithm has to be able to handle not only sphere-sphere contacts, but also sphere-plane and sphere-cylinder contacts. One can easily verify that if planes and cylinders with infinite moments of inertia are used ($I_1 = \infty$), the same simple contact law can be applied as the one derived here for spheres. (Only in the expression of m_t (Eq. 18) the term \vec{l}_1^2/I_1 is set to zero.)

Many contacts

As we have pointed out, the unilateral frictional problems of contacts cannot be solved independently in a dense granular system. The unknowns of one contact $\vec{\mathcal{R}}^{\text{new}}$ and $\vec{\mathcal{V}}^{\text{new}}$ depend on adjacent “new” contact forces that are also unknown. In this way a contact force is coupled to every other contact if they are connected through the contact network. This is a natural consequence of the perfect rigidity, e.g. a collision can immediately affect the forces even in a very far part of the system.

In order to solve this global multi-contact problem, i.e. to satisfy the constraint conditions for all contacts, an iterative method is applied in CD. This *iterative solver* is executed at every time step before the implicit Euler integration can proceed one step further with the newly provided forces.

This method works as follows. At each iteration step we update every contact, independently in the sense that for one contact-candidate a “new” contact force is calculated based on a one-contact shock law, pretending that the current forces of the neighboring contacts are constant. After that the resulting force is stored immediately as the current force of the given contact and a new candidate is chosen for the next update. In that way all the contact forces are updated one by one sequentially, which of course does not yet provide a global solution, but approaches it to some extent. Then this iteration step is repeated many times letting the forces relax according to their neighborhood towards a globally consistent state. After satisfactory convergence is reached the iteration loop is stopped. With convergence we mean that further update of the contact forces gives only negligible changes, thus the constraint conditions are practically fulfilled for the whole system.

If the inelastic shock law is applied for the one-contact update, one must not forget that the forces from the adjacent particles (acting now as external forces) exert also torques \vec{T}_0^{ext} and \vec{T}_1^{ext} , that have to be involved by the generalized vector \mathbf{F}^{ext} in Eq. (5), where the two torques originally were set to zero.

In contrast to this sequential process a simple parallel update would be unstable. Regarding the order of the update sequence within the list of the candidates, it is preferably random and the random pattern is generated repeatedly for each sweep. In this way we want to avoid any bias in the information spreading, what may be caused e.g. by geometrical sweeps. (If the update order is from top to the bottom, the news of a collision or other events pass faster through the contact network downwards than upwards, at least in the early stage of the iteration process.) It has to be mentioned that the *random sweep* described here differs from the well known *random sequential update* because while in this latter the choice of a contact is independent from the previous choices (the same contact could be selected even three times successively), the *random sweep* selects each contact exactly once within one iteration step.

In applications the iteration process of the *contact dynamics* has a nice behavior and converges under reasonable assumptions. About the conditions of convergence more can be found in [6] and references therein.

Convergence criteria

Convergence criteria [16] are applied in the iteration loop to decide, whether the force-system has reached a satisfactory consistent state or further iterations are needed. That is, a convergence criterion is a rule according to which one chooses the final number of the iterations within one time step. Various criteria are used by different research groups, but the structure or efficiency of these criteria is not much discussed in the literature.

In the following a few possible choices are presented, where the first two examples make conditions on the relative change of the forces. The notations used here are the following: $\vec{\mathcal{R}}_\alpha$ is the force of the contact-candidate α in the current state of the iteration process, $\Delta\vec{\mathcal{R}}_\alpha$ is its change during the last iteration step and the brackets $\langle \rangle$ mean average over all candidates.

The first local criterion is:

$$\left| \Delta \vec{\mathcal{R}}_\alpha \right| \leq \varepsilon \left| \vec{\mathcal{R}}_\alpha \right| , \quad (35)$$

which inequality is required for every α . Once it is satisfied everywhere, the iteration loop stops. With the parameter ε the required accuracy can be given. With smaller ε the calculation is more accurate, but the loop of the iteration is forced to run longer. However, if this criterion is applied, an additional cutoff for small forces is needed because small numerical fluctuations present in the simulation can be relatively large for tiny contact forces (there are always such forces in large granular packings), and therefore condition (35) cannot be fulfilled. One way to solve this is to add a certain small force δ to the right hand side.

The second example is of global type:

$$\Delta \left\langle \left| \vec{\mathcal{R}}_\alpha \right| \right\rangle \leq \varepsilon \left\langle \left| \vec{\mathcal{R}}_\alpha \right| \right\rangle . \quad (36)$$

Here the change in the average force is tested, thus it means only one condition globally for the whole system. The role of ε is the same as in the local case, but of course the same value of ε provides different accuracies for the calculation of the force-system.

We performed test runs [17] in order to compare the efficiency of the two criteria. Here the extent of the errors and the average iteration over many time steps needed by the simulation were measured, this latter representing the computational effort. In most cases the exact solution to the forces was not available, so one cannot describe the errors as differences between exact and approximate solutions. Here the level of accuracy was simply characterized by the average overlap, what should be zero in an ideal case. This non-extensive investigation provided the results that both criteria are working well, but in many cases significant differences in the efficiency were found. However, which criterion is more efficient depends on the specific situation and also on the required level of accuracy.

Finally we mention the example that a criterion can simply prescribe a fixed number of iterations:

$$N_I = \text{const}, \quad (37)$$

i.e. at every time step the iteration loop stops after N_I steps. The accuracy can be improved here by applying larger N_I number. This choice of the criterion behaves also nicely in simulations and one of its advantages is simplicity, which makes the operations of the program more transparent giving the possibility of a better understanding of the method.

Sources of errors

When numerical simulations are performed, numerous simplifications and approximations are needed, which lead to dynamics somewhat different from that in a real system. These can be e.g. the assumption of point-contacts or constraint conditions when setting up a theoretical model of a real system, or other type of approximations due to the numerical implementation of this theoretical model, e.g. a discrete integration scheme.

Knowing about the trivial sources of deviations, one can formulate a reduced expectation from the algorithm (as we did in this section): “We want to have a dynamics based on the implicit Euler integration, where the contact forces satisfy the Signorini and Coulomb conditions.”

Is this requirement met by the here presented algorithm? In fact, the computation of contact forces can lead to further errors. The first and main reason of this is that the convergence of the iterative process is not perfect, the loop is necessarily broken after finitely many steps. More about the consequences of this non-accurate force calculation can be found in the next section. Additional errors can emerge even if the one-contact shock law is satisfied everywhere in the system. This is because in the shock law some geometrical changes are neglected when predicting the “new” configuration. E.g., for approaching particles the contact normal can slightly turn or the vectors \vec{l}_0, \vec{l}_1 can suffer small changes, which would alter the matrix \mathbf{H} . However, if the relative displacement of the particles during one time step is small compared to the particle size and to the curvature of the contacting surfaces, these geometrical changes are kept also small and their effect can be typically neglected.

SPURIOUS ELASTIC BEHAVIOR

This section is devoted to the behavior of *contact dynamics* arising from the iterative force computation and to its consequences. The study of the algorithm is carried out in a manner commonly applied in physics: starting with the given microscopic laws (e.g. the one-contact shock law here) properties of global behavior are examined. For a simple test system a coarse grained description is given based on the discrete dynamics, where physical phenomena such as diffusion or sound propagation will turn out to be relevant.

Relaxation of the contact forces

In order to learn more about CD, one can analyze and test the algorithm using the following very simple system [18]. The system consists of an array of identical rigid disks or spheres aligned in a straight line (Fig. 4) and is considered one-dimensional, as only the motion along the line is taken into account (spinning or transversal motion is not allowed). The long chain of particles is compressed by external forces acting at the ends, the inner part of the chain is free from external forces. The neighboring particles are permanently in contact, i.e. $g_i^{\text{pos}} = 0$, where the i th contact is between the particles i and $i + 1$. In this one-dimensional case the tangential forces are zero and the normal contact forces are denoted by \mathcal{R}_i . First we show how the *iterative solver* works for this simple case.

For the update of the contact forces the shock law (34) is applied. Provided the particles remain in contact and no friction is considered, the update of the i th contact attains the following form:

$$\mathcal{R}_i := \frac{m}{2\Delta t} (v_i - v_{i+1}) + \frac{\mathcal{R}_{i-1} + \mathcal{R}_{i+1}}{2} . \quad (38)$$

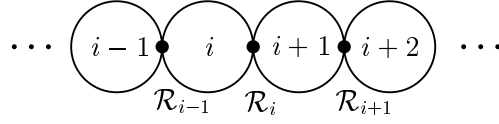


FIGURE 4. A multi-contact situation in a 1D array. External forces act only on particles far away from those shown. Each particle is subjected only to the contact forces of the adjacent ones.

Based on the current values of the adjacent velocities and forces, a new value of \mathcal{R}_i is given by this assignment which is applied several times on the contacts in the way we described before for the multi-contact states. Here, the effective mass (the normal inertia of the contacts) is half of the particle mass m .

As we are searching for a continuum description, the shock formula (38) can be regarded as the discretized form of a partial differential equation (PDE). In order to make this transformation, on one hand, we consider the particle index i as space variable x and replace the differences of consecutive quantities by spacial derivatives in the usual way:

$$\frac{v_{i+1} - v_i}{d} \rightarrow \partial_x v \quad (39)$$

and

$$\frac{\mathcal{R}_{i+1} + \mathcal{R}_{i-1} - 2\mathcal{R}_i}{d^2} \rightarrow \partial_x^2 \mathcal{R} , \quad (40)$$

where d is the particle diameter. On the other hand we introduce a fictitious time t^* for the iteration process, to be able to describe the force evolution. (Note that the physical time does not elapse while the iterations develop the forces.) Then the force change $\Delta \mathcal{R}$ during one iteration step Δt^* can be replaced by a time derivative:

$$\frac{\Delta \mathcal{R}}{\Delta t^*} \rightarrow \partial_{t^*} \mathcal{R} . \quad (41)$$

Thus, by applying these transformations straightforward to the assignment (38) one arrives to the following PDE:

$$\partial_{t^*} \mathcal{R} = D \partial_x^2 \mathcal{R} - \beta \partial_x v \quad (42)$$

$$\text{with } D = q \frac{d^2}{\Delta t^*} , \quad (43)$$

$$\beta = q \frac{md}{\Delta t \Delta t^*} , \quad (44)$$

$$\text{and } q = \frac{1}{2} . \quad (45)$$

This analytic form clearly reveals the nature of the iteration loop: The contact forces relax towards the solution in a diffusive way. (The term $\partial_x v$ being constant during the iteration depends only on x but not on t^* .)

The introduction of the constant q reflects a subtlety regarding the sequential character of the update which was not taken into account in the derivation of Eqs.(42,43,44,45). In fact, $q = 1/2$ corresponds to a parallel update, but the right hand side of Eq.(38) always employs the freshly updated values \mathcal{R}_i , not those from the beginning of the iteration sweep. However, it can be shown that a calculation based on the random sweep update instead of a parallel one results in the same form of the PDE, only the value of q is renormalized:

$$q = \frac{4\sqrt{e} - 5}{2} \approx 0.797 \quad (46)$$

(for the derivation see [18]).

The diffusion like relaxation of the forces has an important consequence concerning the number of iterations N_I which is also crucial for the efficiency of the algorithm, as the computational time is mainly expended to the iterative force calculation. Due to the diffusive behavior a long iteration process can be expected e.g. when an external force changes or a collision occurs at one end of the array. One can estimate the number of iterations required to reach an “equilibrium” state (convergence) for the forces in the whole system, where the estimation is based on the relation of two characteristic lengths: the diffusion length related to N_I steps

$$l_{\text{diff}} = \sqrt{4D\Delta t^* N_I} \quad (47)$$

must be much larger than the system size L . This implies the following estimation (q is being of order 1)

$$N_I > (L/d)^2, \quad (48)$$

that is N_I scales with the square of the linear system size.

One can expect similar diffusive relaxation in dense two and three-dimensional systems, where the diffusion takes place in a complex contact network instead of a line, still the diffusion length is proportional to $\sqrt{N_I}$ in typical homogen situations. Let us estimate the total number of the contact updates during the force calculation, which represents the computational effort of one timestep T_{CDstep} , where the question is the scaling with respect to the number of particles n . Within one sweep one update is performed for each contact, which implies an update number proportional to n (assuming the average coordination number does not change with n). Therefore the computational time of one time step is given by nN_I apart from a constant factor which results in the following scaling with the particle number:

$$T_{\text{CDstep}} \sim n^2 \quad \text{in 2D} \quad (49)$$

$$T_{\text{CDstep}} \sim n^{5/3} \quad \text{in 3D} \quad (50)$$

(as long as $L^2 \sim n$ in 2D and $L^3 \sim n$ in 3D). For comparison in soft particle MD the computational time of one time step scales like n . Thus applying the CD method in that

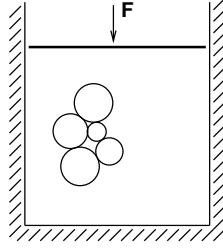


FIGURE 5. Setup of a numerical experiment in two dimensions. A dense packing of 1000 disks is prepared in a container via compressing the system by means of the mobile upper wall.

way, it is computationally more costly for large systems. This is the price for simulating rigid particles without getting elasticity artifacts, which cannot be done with MD.

It is possible to achieve linear scaling with CD reducing the accuracy of the force computation, however, that involves finite stiffness of the particles. As an example let us imagine a CD simulation of a two dimensional dense granular packing, like the one shown in Fig. 5, compressed in a container with an external force acting upon the mobile upper piston. Let us suppose that the system is in equilibrium when the piston force is increased abruptly with ΔF . At the given time step the CD algorithm starts the iterative solver to find the new force system. What happens if one stops the iteration loop before the convergence and performs the time step with the inaccurate forces? The momentum $\Delta F \Delta t$ is transmitted from the piston through the contact forces but only into a depth given by the diffusion length. If N_I was chosen in a way that the corresponding diffusion length is smaller than the system height, than this momentum doesn't reach the fixed base and consequently the upper part of the system is accelerated downwards even if it violates the volume exclusion of the particles. We will show (based on [18]) that the resulting artificial dynamics can be interpreted as the dynamics of soft particles.

Sound waves

Coming back to the one dimensional system, the discrete time-evolution of the velocities can also be transformed into a PDE in a similar manner as it was done for the iteration loop. The Euler scheme (2) gives the following update formula:

$$v_i(t + \Delta t) := v_i(t) + \frac{\mathcal{R}_{i-1}(t + \Delta t) - \mathcal{R}_i(t + \Delta t)}{m} \Delta t, \quad (51)$$

and changing the differences into derivatives the continuum version is:

$$\partial_t v = -\frac{d}{m} \partial_x \mathcal{R}. \quad (52)$$

This equation describes the time-evolution of the velocities on large time and length scales. To connect it to the force update we must relate the “iteration time” t^* to the physical time t . Although, depending on the convergence criterion, there can be in

principle a varying number of iterations during one physical time step Δt , we assume for simplicity that the simple criterion (37) is applied, i.e. the number N_I is fixed.

Hence, with $\Delta t = N_I \Delta t^*$, we can express the above quantities in terms of physical time:

$$\partial_t \mathcal{R} = D \partial_x^2 \mathcal{R} - \beta \partial_x v, \quad (53)$$

$$\text{and } D = q N_I \frac{d^2}{\Delta t} \quad (54)$$

$$\beta = q N_I \frac{m d}{\Delta t^2}. \quad (55)$$

With the equations (52) and (53) we obtained two coupled PDEs. We can combine them to arrive at a wave equation with an additional damping term:

$$\partial_t^2 \mathcal{R} = c^2 \partial_x^2 \mathcal{R} + \partial_t (D \partial_x^2 \mathcal{R}). \quad (56)$$

The sound velocity appearing is of finite value

$$c = \sqrt{q N_I} \frac{d}{\Delta t}. \quad (57)$$

The equation (56) indicates that the CD simulation of the particle chain can lead to sound propagation like in an elastic medium, though the one-contact force update assumes perfectly rigid and completely inelastic contacts. This deviation from the original hard particle model, as it was mentioned before, originates from the incomplete relaxation of the forces. As a consequence, small N_I yields systematic errors in the force calculation and involves soft particles in the sense that the particles can overlap, furthermore, the time evolution of these overlaps corresponds to elastic waves. The sound velocity is proportional to $\sqrt{N_I}$, which goes to infinity in the limit of infinite N_I , as it should for rigid particles.

Searching for the dispersion relation one can perform a Fourier transformation on Eq. (56) and obtain the properties of the different wave modes. The oscillation frequency ω of the wave number k is

$$\omega(k) = k \sqrt{c^2 - \frac{D^2 k^2}{4}}. \quad (58)$$

That means, $\omega(k)$ becomes zero at a critical wave number

$$k_c = \frac{2c}{D} \sim \frac{1}{\sqrt{N_I}}, \quad (59)$$

and waves with k larger than k_c (short wave lengths) are over-damped. The damping time $\tau(k)$ for the oscillating modes is given by:

$$\tau(k) = \frac{2}{D k^2}. \quad (60)$$

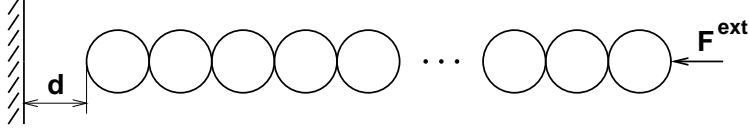


FIGURE 6. Initial configuration of a numerical experiment for testing properties of artificial sound waves.

We derived the dispersion relation (58) in the continuum limit which is a good approximation for small wave numbers, but not close to the border of the Brillouin zone ($k_{\text{Br}} = 2\pi/d$), where the effect of the spatial discreteness cannot be neglected. However, increasing the number of the iterations sufficiently, k_c becomes small compared to k_{Br} . Actually, for $N_I \geq 10$ the formula (58) works well not only for small wave numbers but for all oscillating modes, as can be verified numerically.

Related to the sound velocity and the dispersion relation one can define the following characteristic lengths:

$$l_{\text{sound}} = c \Delta t \quad (61)$$

is the distance the sound can travel during one time step and

$$\lambda_c = \frac{2\pi}{k_c} \quad (62)$$

is the wave length of the largest overdamped mode. If l_{sound} and λ_c are chosen much larger than the system length L (with proper choice of N_I), the elasticity artifacts are avoided. This is the same length-scale as defined by the diffusion length:

$$l_{\text{diff}} = \sqrt{4D\Delta t}, \quad (63)$$

since all three lengths are of the same order of magnitude: $\mathcal{O}(d\sqrt{qN_I})$. If the system is too large compared to N_I in the sense that $L > l_{\text{diff}}(N_I)$ the simulation involves artificial elasticity.

Numerical confirmation

1D simulation

In order to confirm the results of the coarse grained description, we performed the following numerical experiment: The starting configuration of the simulation consists of an array of 50 disks and an immobile wall, the geometry can be seen in Fig. 6. Initially the gap between the wall and the leftmost particle is one disk diameter (d), the gap between the particles is zero and the array has zero velocity. Starting from $t = 0$ a constant external force (F^{ext}) is applied on the rightmost particle which accelerates the array towards the wall (only horizontal motions are present). As simulation parameters we chose $N_I = 40$ and $F^{\text{ext}} = 0.05 dm\Delta t^{-2}$.

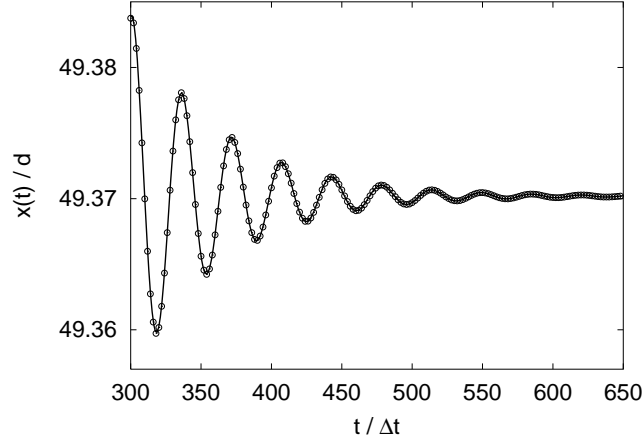


FIGURE 7. Damped oscillation in a Contact Dynamics simulation. The dots indicate the measured data: the position of the rightmost particle versus time (for details see the text). The line is an exponentially damped sine function, where the frequency and the damping time is provided by the continuum model.

The collision with the wall induces a relative motion of the grains and generates sound waves in the array. After a transient period the grains remain permanently in contact (the whole array is pressed against the wall by F^{ext}). Since the different wave modes have different relaxation time, after a while only the largest wave length mode survives. This wave length is four times the system size because the wall represents a fixed boundary while the right side is free. Since the wave length is given the oscillating frequency and the damping time can be calculated from Eq. (58) and Eq. (60). For comparison with the simulation we measured the motion of the rightmost particle. The expected motion is a damped oscillation

$$x(t) = x_0 + A \exp(-t/\tau) \sin(\omega t + \phi) , \quad (64)$$

where the parameters x_0 , A and ϕ are the offset, the amplitude and the phase shift respectively. The Figure 7 shows the measured data (dots) and the fitted curve (64) using the calculated values of ω and τ . It shows that the simulation agrees with the coarse grained description very well.

2D simulation

After the analysis of the regular 1D system the important question arises whether its behavior is relevant for higher dimensions and for less regular systems. In CD simulations of two-dimensional random packings of disks the same “elastic” waves can be observed (even transversal modes were found).

The simulation presented here corresponds to the thought-experiment of the two-dimensional random dense packing we discussed before Fig. 5. It consists of 1000 disks with radii distributed uniformly between r_{\min} and $r_{\max} = 2r_{\min}$, the mass of each disk being proportional to its area. The base and the two side-walls are fixed while the upper

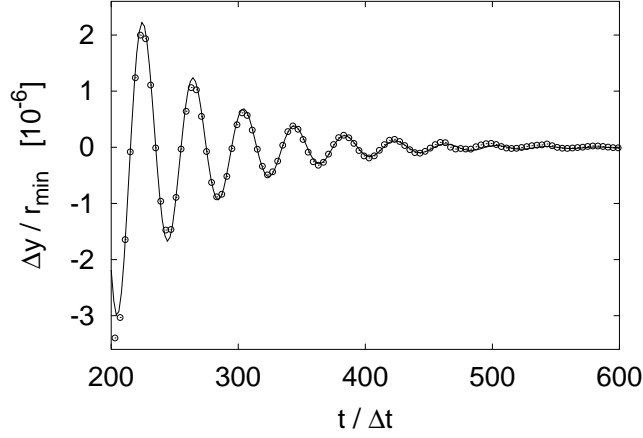


FIGURE 8. Oscillations in a 2D simulation are similar to the 1D case. Here the sound waves are generated in a random dense packing of disks. The dots are the measured position of the upper wall versus time (see Fig. 5), while the curve is a fitted exponentially damped sine function.

piston is mobile. Starting from a loose state, we compressed the system and waited until the packing reached an equilibrium state (the compression force F applied on the piston was kept constant). The simulation was carried out without gravity and with a Coulomb friction coefficient of 0.05 for all the disk-disk and disk-wall contacts.

After the packing was relaxed completely, we generated sound waves by increasing the compression force abruptly to $F + \Delta F$. After a transient period only one standing wave mode survives (both the wavenumber vector and the collective motion are vertical), where the piston, representing a free boundary, oscillates with a relatively large amplitude. We measured the vertical position of the piston versus time and found that the data can be fitted by an exponentially damped sine function (Fig. 8). Here, in contrast to the 1D case, also ω and τ are fit parameters, since, due to the different geometry, the values (58) and (60) cannot be adopted. As the system has random structure, a more complex treatment is required for a quantitative description. However, we checked the most important relation, namely that the scaling properties of ω and τ remain valid also for the 2D random system, that is $\omega \sim \sqrt{N_I}$ and $\tau \sim N_I^{-1}$, which means that the artificial visco-elasticity of the particles depends on the number of iterations in the same manner as we showed for the 1D chain.

Global elasticity

It is instructive to compare our test-system to its simplest MD counterpart where the contact forces depend linearly on the local kinematic variables, i.e. the so called *linear spring/dashpot model*

$$\mathcal{R}_i = -\kappa(x_{i+1} - x_i - d) - \gamma(v_{i+1} - v_i) \quad (65)$$

with the spring stiffness κ and the damping coefficient γ . Searching again for the large scale behavior of the particle chain one arrives to the same PDE as in Eq. (53) with its

coefficients being inherited from Eq. (65):

$$\partial_t \mathcal{R} = \frac{\gamma d^2}{m} \partial_x^2 \mathcal{R} - \kappa d \partial_x v \quad (66)$$

This allows us to relate the physical MD model parameters to the “technical” CD parameters (N_I and Δt):

$$\kappa = qm \frac{N_I}{\Delta t^2} \quad (67)$$

and

$$\gamma = qm \frac{N_I}{\Delta t} \quad (68)$$

This equivalence shows that on large scales the CD chain should behave identical to its MD counterpart, e.g. it will indeed exhibit a global shrinkage proportional to an external compressive load. Note that a real congruence can be expected only for the collective behavior but not on the level of contacts. In the CD method, as explained above, contact forces are not related to the overlaps. Overlaps are present merely due to the incompleteness of the force-calculation and in fact are stochastic quantities because of our random update procedure. Only on scales larger than the grain size, where the fluctuations of these local “deformations” are averaged out, the behavior can be smooth as in an elastic medium (shown e.g. in Fig. 7).

Performing simulations within the scope of the spurious elasticity (i.e. $l_{\text{diff}} < L$) Equations (67) and (68) provide the effective stiffness and viscous dissipation of contacts. One can see that the stiffness depends on N_I , but not on the total number of particles n . Therefore the choice of a constant N_I independently from n provides the same stiffness, no matter how large the system is. Using the CD in that way, the superlinear scaling of the computational time in Eq. (49) and Eq. (50) can be avoided. Thus

$$T_{\text{CDstep}} \sim n, \quad (69)$$

similarly to MD. In this case, of course, elasticity artifacts (sound waves, elastic deformations) are involved by the dynamics.

Interestingly, the reduction of N_I and Δt while $N_I/\Delta t$ is kept constant increases the stiffness, but does not affect the value of the dissipation γ or the total number of updates corresponding to a given physical time interval. Hence, it seems to be worth reducing N_I and Δt in that way (at least to some degree) if the goal is to simulate harder particles.

The results concerning the iteration process made it possible to characterize CD simulations by means of the diffusion length. One can draw a distinction between two different types of behavior: spurious soft region for small values of l_{diff} , and rigid region for large values of l_{diff} , where the transition can be found around the linear system size. We would like to emphasize, however, that only dense systems were considered so far, such states where roughly the whole system is one large cluster of contacting particles. In loose situations, where mainly free particles or small separate clusters are present, the

system size is not relevant. Here, in order to avoid the soft region, one has to compare l_{diff} to the size of the largest cluster.

The description of the test system was based on the assumption of a constant number of iterations for every time step, and due to this premise the analytical treatment became simple and directly comparable to the corresponding simulation. It is important, though, that applications of other convergence criteria typically involve fluctuating N_I (i.e. it can vary from time step to time step), and therefore steps with different “stiffness” are mixed during the integration of motion. Consequently, the behavior of the CD method can be more complex in detail, but qualitatively the results of constant N_I remain relevant also here. For example, the mechanism resulting in soft particles is the same, or shock-waves with finite velocity can also arise in the case of fluctuating N_I in a similar way.

SUMMARY

We presented a 3D contact dynamics algorithm in detail to simulate large systems of rigid spherical particles and gave a review of the iterative force calculation, where the perfect volume exclusion and the exact Coulomb’s law of dry friction are adopted. We showed that the systematic errors can lead to a spurious collective elastic behavior and reproduced the numerical results analytically for a simple test system.

Besides elucidating the origin of elastic behavior, the coarse grained description revealed important characteristics of the CD method. It was shown that using the iterative solver the contact forces are approached in a diffusion like manner, which is a crucial information concerning the computational time, when simulating rigid particles properly.

When lowering the accuracy of the force calculation, CD simulation involves soft particles. In that way Coulombian friction can be combined with global elasticity easily and considerable computational time can be saved: even better performance than MD can be achieved.

ACKNOWLEDGMENTS

The authors thank G. Bartels, L. Brendel, D. Kadau and D. E. Wolf for valuable discussions. Thanks are due to APS for kind permission of reproducing figures. This work was supported by OTKA T029985, T035028.

REFERENCES

1. Cundall, P. A., and Strack, O. D. L., *Géotechnique*, **29**, 47–65 (1979).
2. Wolf, D. E., “Modeling and Computer Simulation of Granular Media,” in *Computational Physics*, edited by K. H. Hoffmann and M. Schreiber, Springer, Berlin, 1996.
3. McNamara, S., and Young, W. R., *Phys. Rev. E*, **50**, R28–R31 (1994).
4. Jean, M., and Moreau, J. J., “Unilaterality and dry friction in the dynamics of rigid body collections,” in *Proceedings of Contact Mechanics International Symposium*, Presses Polytechniques et Universitaires Romandes, Lausanne, Switzerland, 1992, pp. 31–48.

5. Moreau, J. J., *Eur. J. Mech. A-Solids*, **13**, 93–114 (1994).
6. Jean, M., *Comput. Methods Appl. Mech. Engrg.*, **177**, 235–257 (1999).
7. Daudon, D., Lanier, J., and Jean, M., “A micro mechanical comparison between experimental results and numerical simulation of a biaxial test on 2D granular material,” in *Powders & Grains 97*, Balkema, Rotterdam, 1997, p. 219.
8. Radjai, F., Roux, S., and Moreau, J., *Chaos*, **9**, 544–550 (1999).
9. Nouguié-Lehon, C., Dubujet, P., and Cambou, B., Analysis of granular material behaviour from two kinds of numerical modelling (2002), 15th ASCE Engineering Mechanics Conference.
10. Radjai, F., Jean, M., Moreau, J., and Roux, S., *Phys. Rev. Lett.*, **77**, 274–277 (1996).
11. Radjai, F., Wolf, D., Jean, M., and Moreau, J., *Phys. Rev. Lett.*, **80**, 61–64 (1998).
12. Staron, L., Vilotte, J., and Radjai, F., *Phys. Rev. Lett.*, **89**, 204302–204305 (2002).
13. Kadau, D., Bartels, G., Brendel, L., and Wolf, D., Pore stabilization in cohesive granular systems (2002), cond-mat/0206572, submitted to Phase Transitions.
14. Kadau, D., Bartels, G., Brendel, L., and Wolf, D. E., *Comp. Phys. Comm.*, **147**, 190–193 (2002).
15. Moreau, J., and Panagiotopoulos, P., *Nonsmooth Mechanics and Applications*, Springer, Vienna, 1988.
16. Bartels, G., *Die Kontakt-Dynamik Methode*, Master’s thesis, Gerhard Mercator University, Duisburg, Germany (2001).
17. Bartels, G., Unger, T., and Wolf, D., Comparison of convergence criteria in contact dynamics simulations (2001), unpublished.
18. Unger, T., Brendel, L., Wolf, D. E., and Kertész, J., *Phys. Rev. E*, **65**, 061305 (2002).